RNA Biology

ISSN: 1547-6286 (Print) 1555-8584 (Online) Journal homepage: https://www.tandfonline.com/loi/krnb20

Regulation of the Ysh1 endonuclease of the mRNA cleavage/polyadenylation complex by ubiquitin-mediated degradation

Susan D. Lee, Hui-Yun Liu, Joel H. Graber, Daniel Heller-Trulli, Katarzyna Kaczmarek Michaels, Juan Francisco Cerezo & Claire L. Moore

To cite this article: Susan D. Lee, Hui-Yun Liu, Joel H. Graber, Daniel Heller-Trulli, Katarzyna Kaczmarek Michaels, Juan Francisco Cerezo & Claire L. Moore (2020) Regulation of the Ysh1 endonuclease of the mRNA cleavage/polyadenylation complex by ubiquitin-mediated degradation, RNA Biology, 17:5, 689-702, DOI: 10.1080/15476286.2020.1724717

To link to this article: https://doi.org/10.1080/15476286.2020.1724717

View supplementary material

Published online: 12 Feb 2020.

Submit your article to this journal

Article views: 390

View related articles

View Crossmark data

Citing articles: 2 View citing articles

Full Terms & Conditions of access and use can be found at
https://www.tandfonline.com/action/journalInformation?journalCode=krnb20

RNA BIOLOGY
2020, VOL. 17, NO. 5, 689–702
https://doi.org/10.1080/15476286.2020.1724717

Taylor & Francis
Taylor & Francis Group

RESEARCH PAPER

Check for updates

Regulation of the Ysh1 endonuclease of the mRNA cleavage/polyadenylation complex by ubiquitin-mediated degradation

Susan D. Lee[a], Hui-Yun Liu[a], Joel H. Graber[b], Daniel Heller-Trulli[a], Katarzyna Kaczmarek Michaels[a], Juan Francisco Cerezo[c], and Claire L. Moore[a]

[a]Department of Developmental, Molecular, and Chemical Biology and Tufts School of Graduate Biomedical Science, Tufts University School of Medicine, Boston, MA, USA; [b]Computational Biology and Bioinformatics Core, Mount Desert Island Biological Laboratory, Bar Harbor, ME, USA; [c]Experimental Sciences, Universidad Francisco de Vitoria, Madrid, Spain

ABSTRACT

Mutation of the essential yeast protein Ipa1 has previously been demonstrated to cause defects in pre-mRNA 3′ end processing and growth, but the mechanism underlying these defects was not clear. In this study, we show that the *ipa1-1* mutation causes a striking depletion of Ysh1, the evolutionarily conserved endonuclease subunit of the 19-subunit mRNA Cleavage/Polyadenylation (C/P) complex, but does not decrease other C/P subunits. *YSH1* overexpression rescues both the growth and 3′ end processing defects of the *ipa1-1* mutant. *YSH1* mRNA level is unchanged in *ipa1-1* cells, and proteasome inactivation prevents Ysh1 loss and causes accumulation of ubiquitinated Ysh1. Ysh1 ubiquitination is mediated by the Ubc4 ubiquitin-conjugating enzyme and Mpe1, which in addition to its function in C/P, is also a RING ubiquitin ligase. In summary, Ipa1 affects mRNA processing by controlling the availability of the C/P endonuclease and may represent a regulatory mechanism that could be rapidly deployed to facilitate reprogramming of cellular responses.

ARTICLE HISTORY
Received 7 December 2019
Revised 25 January 2020
Accepted 27 January 2020

KEYWORDS
Polyadenylation; ubiquitination; alternative mRNA processing

Introduction

Tight regulation of gene expression is critical for proper cellular function. A step of mRNA synthesis that can influence gene expression is mRNA polyadenylation, an essential maturation step in which mRNA precursor is trimmed by cleavage at its 3′ end and a poly(A) tail added. Regulating the overall efficiency at which this processing occurs is a mechanism by which cells could globally alter the amount of mRNAs that reach the cytoplasm for translation. In a different regulatory strategy, a process known as alternative polyadenylation results in a change in the cleavage site position to yield specific mRNA isoforms with different lengths of 3′ untranslated (3′ UTRs) or coding regions. Shortening of the 3′ UTR removes binding sites for factors that influence mRNA stability, translation, subcellular localization, and partner protein interaction, while coding region shortening alters protein function [1,2]. Alternative polyadenylation plays an important and increasingly appreciated role in regulation of gene expression, and the choice of poly(A) site has been shown to vary with changes in cell state during development, tissue differentiation, tumorigenesis, senescence, and as part of the response to stress or infection [3–17].

Regulation of polyadenylation can be elicited by changing the relative concentration of the core mRNA 3′ end processing factors or their recruitment to RNA Polymerase II (Pol II) elongation complexes, by affecting how quickly Pol II reaches downstream poly(A) sites, and in some cases, by the expression of positive or negative regulators [7,10,12,18]. Post-translational modification of processing factors is another mechanism for regulation of mRNA 3′ end formation. Modifications such as phosphorylation [19–26], acetylation [27], and sumoylation [28] have all been reported to affect the activity of the Cleavage/Polyadenylation (C/P) complex or usage of alternative poly(A) sites. Many studies have also shown that experimental depletion of subunits of the C/P complex can lead to changes in the choice of poly(A) sites (reviewed in [7] and [12]).

In yeast, the C/P complex is composed of CPF, CF IA, and CF IB. CPF contains 14 subunits and includes the enzymes of the complex, which are the Ysh1 endonuclease, the Pap1 poly(A) polymerase, and two phosphatases, Ssu72 and Glc7, which can act on RNA Polymerase II (Pol II). CF IA, which has four subunits (Clp1, Pcf11, Rna14 and Rna15), provides RNA recognition and scaffolding functions to bring together CPF, CF IB, and Pol II. CF IB is the RNA-binding protein Hrp1. The C/P machinery is highly conserved from yeast to mammals [10,29,30], and proteins with sequence, functional, and/or structural homology to almost all of the yeast subunits can be found in the mammalian C/P complex.

While much progress has been made recently to elucidate the composition of the C/P complex and its structural organization [29,30], regulatory mechanisms that lead to changes in levels of C/P subunits are not so well defined. One mechanism that has been described is regulation of the amount of the CF IA subunits Pcf11 and Rna14 and their metazoan homologs PCF11 and CSTF3 by premature transcription

CONTACT Claire L. Moore claire.moore@tufts.edu Department of Developmental, Molecular, and Chemical Biology and Tufts School of Graduate Biomedical Science, Tufts University School of Medicine, Boston, MA 02111, USA

© 2020 Informa UK Limited, trading as Taylor & Francis Group

termination upstream of the gene's stop codon [31]. In addition, alterations in the expression of mRNAs encoding C/P subunits have been reported upon cell differentiation, increased proliferation, or in response to external stimuli [32], but these changes do not always correlate with changes in protein levels [5,33].

The levels of C/P proteins could also be regulated by changes in translation or protein stability. We have previously shown that ubiquitination, a modification that can lead to protein degradation, can modulate C/P efficiency, but molecular targets were not identified [34]. An attractive target for this type of regulation would be the endonuclease (Ysh1 in yeast and CPSF73 in mammals) [35]. The activity of this enzyme initiates mRNA 3′ end processing, and if it is depleted, 3′ ends are not generated for poly(A) addition, and Pol II transcription does not terminate efficiently [36–38].

In this study, we describe how the level of Ysh1 is regulated by ubiquitin-mediated proteasomal degradation. This targeting of Ysh1 is modulated by the presence of Ipa1, an essential protein that was initially discovered as a factor whose genetic interaction profile was very similar to those of mRNA 3′ end processing factors [39]. Ipa1 forms a stable complex with only the Ysh1 and Mpe1 subunits of the C/P complex [39,40]. We have previously shown that the *ipa1-1* mutant allele causes a defect in both the cleavage and poly(A) addition steps of mRNA 3′ end processing in vitro, lengthening of mRNAs in vivo, inefficient transcription termination downstream of poly(A) sites and at snoRNA genes, and poor recruitment of the Pta1 subunit of the C/P complex to the 3′ end of an mRNA gene [39,41]. We now show that Ipa1 exerts its effects on mRNA 3′ end processing by blocking the ubiquitination of Ysh1, a regulatory mechanism that has not previously been reported.

Results

Ysh1 protein level is decreased by Ipa1 mutation

Because the *ipa1-1* phenotypes were reminiscent of those of 3′-end processing mutants, we investigated whether the levels of subunits of the C/P complex were altered in *ipa1-1*. Western blot analysis of whole-cell extract of *ipa1-1* showed most subunits were not affected. However, some subunits (Rna14, Clp1, Cft1, and Swd2) were increased in level (Fig. 1A), while Ysh1 was the only subunit that showed a striking decrease. Thus, the *ipa1-1* mutation alters the stoichiometry of C/P complex subunits in ways that could explain the processing defects.

Recent findings indicate that CPF can be sub-divided into three enzymatic modules: a nuclease module, a phosphatase module (also called APT for Associated with Pta1), and a polymerase module [40,42,43]. To test whether the CPF organization is compromised in *ipa1-1*, we performed a co-immunoprecipitation experiment using wild-type or *ipa1-1* extracts and antibody against Pap1. The composition of immunoprecipitated proteins was assessed by Western blotting with antibodies against subunits of CPF and CF IA. Consistent with the low level of Ysh1 in *ipa1-1* extract, less Ysh1 was incorporated into CPF (Fig. 1B). Mpe1, Pta1, and Ssu72 also showed decreased incorporation into CPF despite normal levels in the *ipa1-1* total extract (Fig. 1B). The loss of these subunits is likely due to low Ysh1 incorporation into CPF as Ysh1 directly interacts with Mpe1 and Pta1, and Pta1 in turn recruits Ssu72 to the processing machinery [42,44,45]. This result supports the proposal of Casanal, et al. [42] that the nuclease module functions as a bridge to connect the polymerase and phosphatase modules. The interactions of Pap1 with Pfs2 and Fip1 were not affected, as would be expected given that Fip1 directly contacts both Pap1 and Pfs2 [46,47]. Furthermore, the cross-factor interaction between CPF and the CF IA subunits Rna14 and Rna15 was not impaired by the *ipa1-1* mutation. Consistent with defects in CPF composition in *ipa1-1*, defects in cleavage and poly(A) addition seen with *in vitro* reactions using the *GAL7* poly(A) site were rescued by addition of TAP-purified CPF to *ipa1-1* extract (Fig. 1C).

The *ipa1-1* mutant bears four point mutations (I109M, K121I, G226E, and D270V). These mutations result in a loss of Ipa1 protein (Fig. 1A), and the I109M and K121I mutations are in a region identified as interacting with Ysh1 by cross-linking mass-spectrometry [40]. The mutant is slow growing compared to wild-type cells at 30°C, and this growth defect is worsened at 37°C (Fig. 1D, left panel). Our previous report had found that the termination defect and the decrease in the amount of Pta1 recruited to the 3′ end of a transcribed gene in vivo in the *ipa1-1* mutant can be abrogated by Ysh1 overexpression [41]. Consistent with this result, supplementing the *ipa1-1* mutant with additional copies of the *YSH1* gene on a low copy plasmid was able to rescue the growth defect observed in *ipa1-1* (Fig. 1D, right panel). These results indicate that the growth defect conferred by *ipa1-1* is in large part due to the low level of Ysh1.

mRNA expression changes in ipa1-1 *support a processing defect due to Ysh1 and Ipa1 deficiency*

We next tested whether the *ipa1-1* mutation altered the efficiency of 3′-end processing in vivo by looking at the level of endogenous transcripts that contain sequence upstream and downstream of the poly(A) sites of *PDC1* and *RPP1B*, which are genes with single poly(A) sites. These transcripts represent RNA that has not been processed and can be detected by RT-qPCR with a primer pair that spans the poly(A) site. In agreement with the defect caused by *ipa1-1* in the in vitro cleavage/polyadenylation reaction, mutation of *IPA1* greatly increased the amount of unprocessed pre-mRNA at the *PDC1* and *RPP1B* poly(A) sites in vivo (Fig. 2A). Overexpression of *YSH1* restored much of the processing at these poly(A) sites, indicating that the depletion of Ysh1 is a major contributor to the *ipa1-1* 3′ end processing defect.

To further explore the link between the *ipa1-1* mutation and a defect in mRNA 3′ end processing, we examined the RNA-seq data sets of Costanzo et al. [39] to determine changes in the mRNA expression profiles of the *ipa1-1* mutant compared to that of two mutants with strong mRNA 3′ end processing defects, *cft2-1* and *pcf11-2* [39]. Cft2 directly contacts Ysh1 in the CPF complex [40], an interaction conserved with the mammalian homologs, CPSF100 and CPSF73 [48], and Pcf11 is a subunit of a different factor, CF IA. For the genes with increased

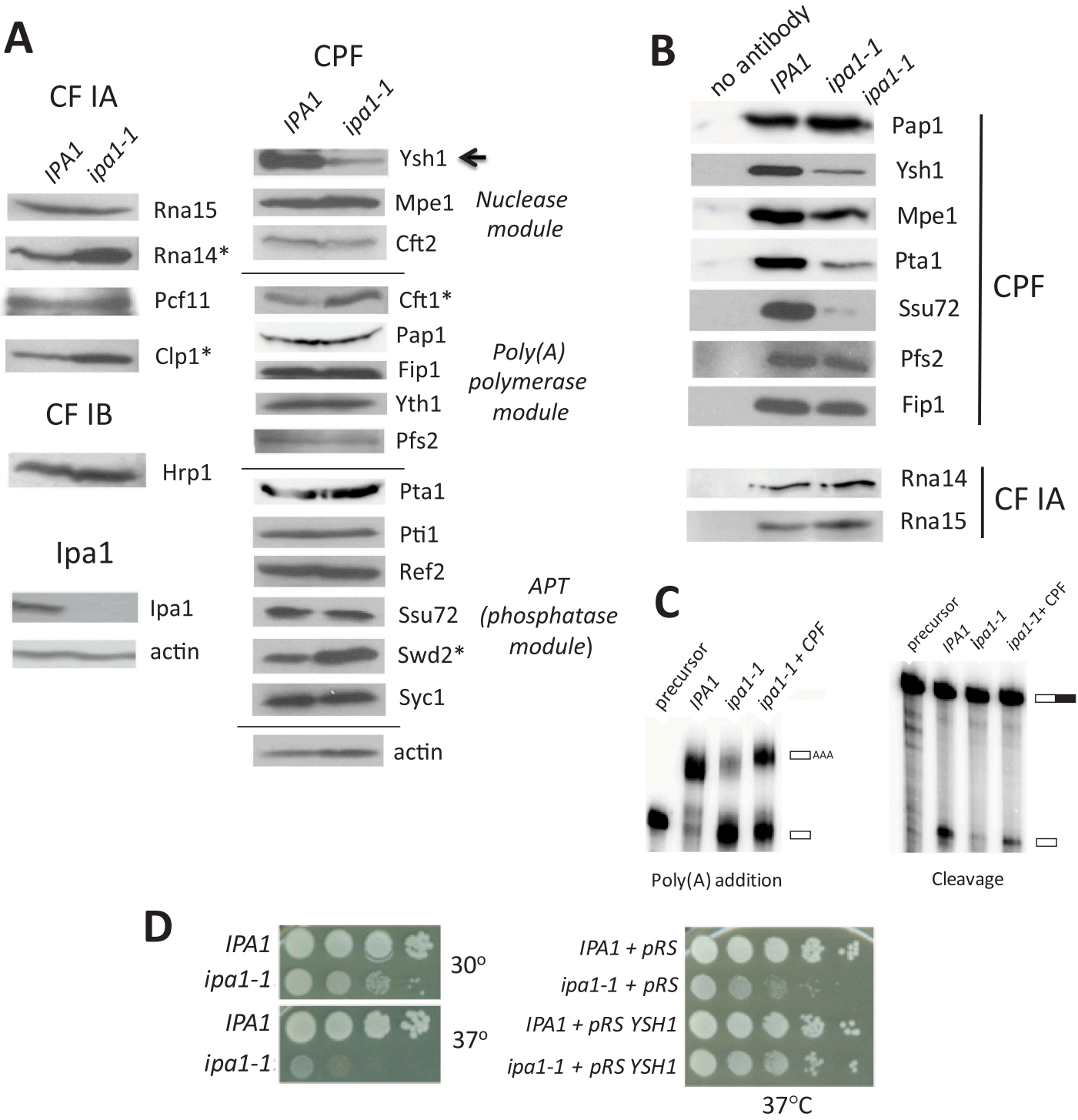

Figure 1. The *ipa1-1* mutant negatively affects CPF stoichiometry, cell growth and mRNA 3′ end processing in vitro.

(A) Expression of subunits of the C/P complex in *IPA1* and *ipa1-1* cells. Cells expressing Myc_{13} tagged Ipa1 were grown at 30°C and shifted to 37°C for 1 hour. Cell extracts were analysed by Western blotting using antibodies against the Myc epitope, C/P subunits, Syc1 (an APT-specific subunit) [43] and actin as a loading control. The Ysh1 subunit (arrow) is decreased in *ipa1-1* cells, and Rna14, Clp1, Cft1 and Swd2 are increased in level (asterisks). **(B)** Interaction of C/P subunits with the poly(A) polymerase Pap1. Co-immunoprecipitation was performed with Pap1 antibody and extract from *IPA1* or *ipa1-1* cells. The eluates were analysed by Western blotting with antibodies against C/P subunits. Pull-down from *IPA1* extract using protein A beads without Pap1 antibody is shown in the left column. **(C)** Cleavage and poly(A) addition activities are rescued by addition of purified CPF to *ipa1-1* extract. Processing extracts were prepared from *IPA1* and *ipa1-1* cells grown at 30°C and then shifted to 37°C for 1 hour. For poly(A) addition, extracts were incubated with ATP and P^{32}-labelled RNA that ends at the *GAL7* poly(A) site. For cleavage-only assays, extracts were incubated with 3′-dATP (a polyadenylation terminator) and P^{32}-labelled RNA containing sequence upstream and downstream of the *GAL7* poly(A) site. RNA products were resolved on a denaturing polyacrylamide gel and visualized with a phosphorimager. Positions of substrate and products are indicated on the right (open rectangles indicate sequence upstream of the cleavage site, the filled rectangle is sequence downstream, and the open rectangle labelled AAA is polyadenylated product). The lane marked 'precursor' indicates the unreacted substrate. **(D)** Relative growth of *IPA1* (wild-type) and *ipa1-1* strains at 30°C and 37°C. For the left panel, cells were grown in liquid YPD, 10-fold serially diluted, spotted onto YPD plates, and incubated for 3 days at the indicated temperatures. For the right panel, cells were transformed with the pRS315 plasmid with or without the *YSH1* gene and spotted on CM-leu plates to maintain selection of the plasmid.

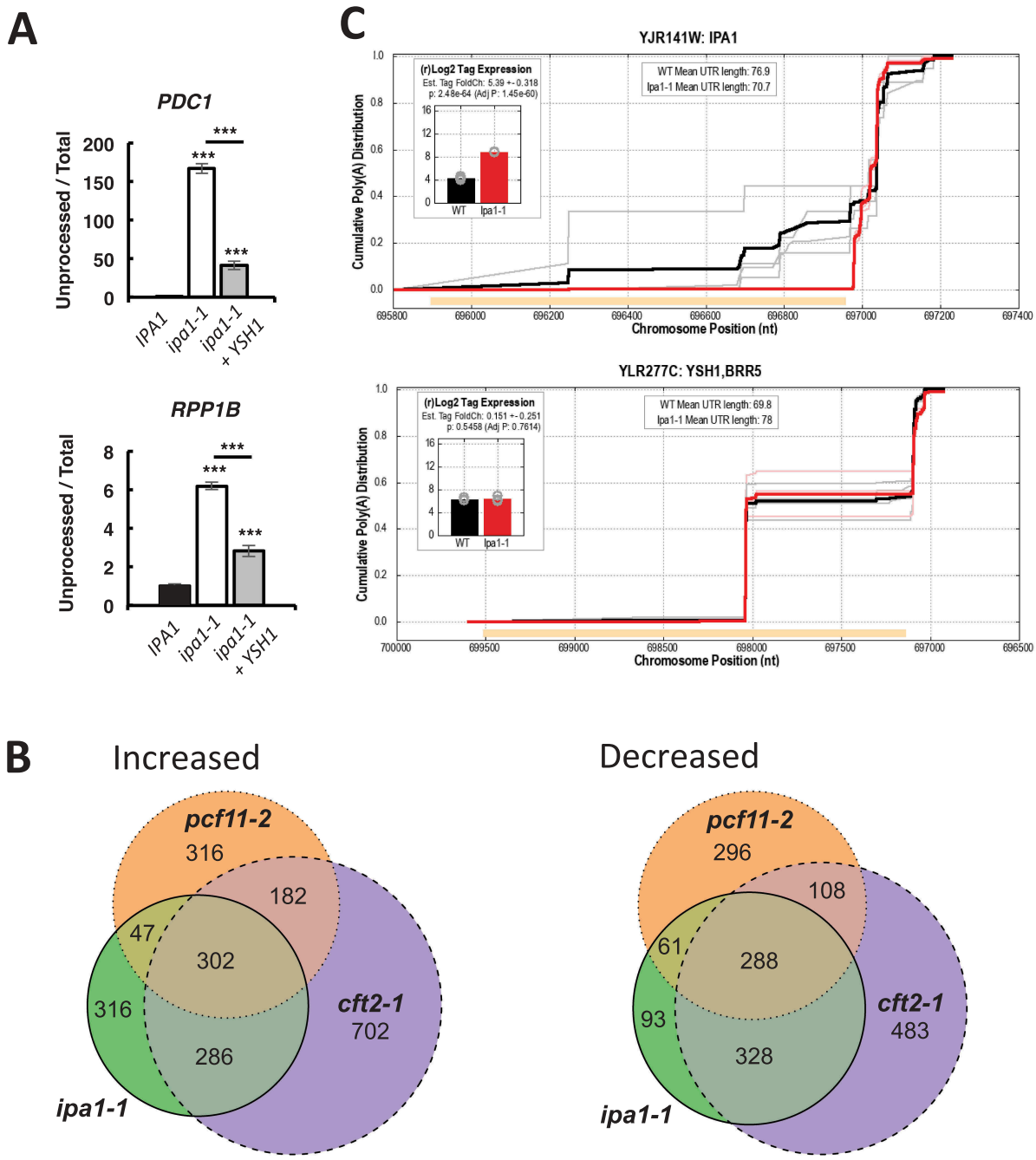

Figure 2. mRNA expression changes support a processing defect due to Ysh1 and Ipa1 deficiency in the *ipa1-1* mutant.

(A) Determination of the level of unprocessed transcripts from the *PDC1* and *RPP1B* genes, as determined by RT-qPCR using primers on either side of the poly(A) site (unprocessed) and a primer pair near the 3′ end of the ORF (total). **(B)** The intersection of genes with increased (left panel, $\log_2$ fold-change > 0.5, *p*-value < 0.2) or decreased (right panel, $\log_2$ fold-change < 0.5, *p*-value < 0.2) expression in each of three mutant strains – *ipa1-1* (green), *pcf11-2* (orange), and *cft2-1* (purple). Expression data were obtained from Costanzo et al. [39] and processed as described in Pearson et al. [41]. **(C)** Cumulative polyadenylation distribution (CPD) plots for the *IPA1 and YSH1* genes for wild-type (black) and *ipa1-1* (red), averaged from three biological replicates each, with traces for individual replicates in grey or pink. The CPD plot [5] shows the empirical likelihood of polyadenylation at or before each position in the gene. Orange bars show coding sequence, with plots oriented such that the direction of transcription is left to right. The inserts show the $\log_2$ tag counts corresponding to mRNAs that are polyadenylated in the 3′ UTR of *IPA1* or *YSH1* for wild-type (black) and *ipa1-1* (red). The $\log_2$ tag counts correspond to reads from the RNA seq data of Costanzo et al. [39], which uses a method that only returns reads from the sequence immediately upstream of poly(A) sites. The sequencing data of Costanzo et al. [39] were also used to obtain the CPD plots.

expression in *ipa1-1*, 73% were shared with those up in *cft2*-1 and 43% with *pcf11-2* (Fig. 2B). Of the genes in *ipa1-1* that are decreased in expression, 80% are shared with those decreased in *cft2-1* and 45% with pcf11-2. The finding that the majority of the *ipa1*-1-sensitive genes are shared with *cft2-1* supports the idea that a major defect in *ipa1-1* is loss of CPF function, and in particular, a defect in the nuclease module of which Ysh1 and Cft2 are part.

Interestingly, when we analysed the sequencing data of Costanzo et al. [39], the *IPA1* mRNA in the *ipa1-1* mutant

showed significantly increased expression (log2 fold-change over wild-type of 5.4) and a suppression of poly(A) sites within the *IPA1* open reading frame (Fig. 2C, top panel). In wild-type cells, ~30% of the IPA1 transcripts end within the ORF, but in ipa1-1, these are completely suppressed, leading to more full-length mRNA isoforms. This observation suggests that the mutant cells are using this mechanism to try to compensate for the loss of the Ipa1 protein (Fig. 1A) and that Ipa1 auto-regulates its own expression.

Ysh1 is degraded via the ubiquitin-proteasome system in ipa1-1

We next investigated the reason for the strong reduction in Ysh1 protein in *ipa1-1*. RNA sequencing analysis of mRNAs in the *ipa1-1* mutant and the isogenic wild-type strain showed no change in *YSH1* mRNA level or shifts in poly(A) site usage (Fig. 2C, bottom panel). Approximately half of the *YSH1* transcripts use a poly(A) site within the coding sequence, but usage of this site does not change in *ipa1-1* (Fig. 2C). We thus considered that the decrease in Ysh1 protein in *ipa1-1* could be attributed to degradation by the ubiquitin-proteasome system. Inactivating the proteasome in the *ipa1-1* strain by deleting the *UMP1* gene, which is needed for efficient proteasome assembly [49], restored the level of Ysh1 to one comparable to that observed in wild-type cells (Fig. 3A). This result suggests that Ysh1 in *ipa1-1* might be post-translationally modified by ubiquitin and targeted for proteasomal degradation. To test this, extracts from strains expressing Myc-tagged Ysh1 were prepared using 2% SDS to disrupt protein–protein interactions, following the protocol described by Laney and Hochstrasser [50] for analysis of ubiquitinated proteins. High molecular weight Ysh1 species were observed in the *ipa1-1 ump1*$^{\Delta}$ cells (Fig. 3B). Similar results were observed if extracts were prepared in 8M urea (Fig. S1A). To further characterize the larger species, Ysh1 was immunoprecipitated from diluted SDS extracts, and immunoprecipitates probed with antibody against ubiquitin or against the Myc epitope on Ysh1 (Fig. 3C). Some of the larger Ysh1 species were lost during the immunoprecipitation, perhaps due to the presence of deubiquitinases in the extract. However, high molecular weight species containing ubiquitin were detected in the precipitate from *ipa1-1 ump1*$^{\Delta}$ cells expressing Myc-Ysh1, but not from *ipa1-1 ump1*$^{\Delta}$ cells lacking the Myc tag or from cells with the unmutated *IPA1* gene (Fig. 3C, lower panel), confirming the accumulation of ubiquitinated Ysh1 when Ipa1 is defective.

Ubiquitination requires the sequential actions of three proteins: E1, the ubiquitin-activating enzyme; E2, a ubiquitin-conjugating enzyme; and E3, a ubiquitin ligase [51,52]. Yeast has only one E1, but multiple E2 and E3 enzymes. To identify E2 and E3 enzymes responsible for Ysh1 ubiquitination in *ipa1-1*, we mutated candidate E2s or E3s in the *ipa1-1* strain and observed Ysh1 protein level. We reasoned that if an enzyme responsible for Ysh1 ubiquitination in *ipa1-1* was not functional, Ysh1 would not be targeted for degradation and would remain at a level comparable to that of wild-type. Mpe1, which is a CPF subunit in the nuclease module, interacts directly with Ysh1 [40] and contains a RING finger-like domain found in one type of E3 ubiquitin ligases [53]. RBBP6, the mammalian homolog of Mpe1, has ubiquitin ligase activity [54,55]. Thus, Mpe1 is a natural candidate for the E3 responsible for Ysh1 ubiquitination. Indeed, when *MPE1* was mutated in *ipa1-1*, Ysh1 protein level was restored to that seen in wild-type cells (Fig. 3D) and growth of *ipa1-1* improved (Fig. 3F), suggesting that this particular E3 is the primary regulator of Ysh1 levels when Ipa1 is defective.

For a candidate E2 enzyme, we focused on Ubc4 because of reported genetic interactions linking Ubc4 with Ipa1 and the C/P machinery. Of the eleven E2 enzymes in *S. cerevisiae* [56], only Ubc4 showed a significant positive genetic interaction with Ipa1 [39], as determined by improved growth when mutations in both *IPA1* and *UBC4* are paired in the same cell. This genetic interaction suggests that Ipa1 action is antagonistic to that of Ubc4. In addition, we had earlier found that the growth defect of the *mpe1-C182G,C185G* mutant was suppressed by overexpression of *HEL2*, encoding a Ring Finger ubiquitin ligase that physically interacts with Ubc4 [34,57,58]. Consistent with these interactions, mutation of *UBC4* restored Ysh1 protein level to a normal level in *ipa1-1* (Fig. 3E) and improved growth of *ipa1-1* (Fig. 3F). Thus, even though Ipa1 has been shown to physically interact with other E2 proteins [59], including Ubc1, Ubc5, Ubc7, Ubc8, Ubc11, Ubc13, and Pex4, the presence of wild-type genes encoding these enzymes or that of the close Ubc4 paralog, Ubc5, is not sufficient to cover for loss of Ubc4 in the *ipa1-1* mutant.

UBC4 and MPE1 are required for in vitro *ubiquitination of Ysh1*

As described above, mutating *UBC4* or *MPE1* in the *ipa1-1* strain restored the Ysh1 level *in vivo*. However, restoration of Ysh1 protein level could be caused by indirect effects of these mutations. Ubc4 functions in various cellular pathways, and because Mpe1 is involved in 3′-end processing, its mutation could affect gene expression of relevant factors. Thus, we developed an *in vitro* ubiquitination assay to investigate whether Ubc4 and Mpe1 are directly involved in Ysh1 ubiquitination. Extracts were made from either wild type or mutant cells and incubated with ubiquitin and CPF purified from yeast expressing 3xHA-TAP-tagged *YSH1* in the *mpe1-1* mutation, which causes Mpe1 to dissociate from CPF [53]. We were unable to purify Ysh1 alone as we have found that it is prone to aggregation.

Using anti-HA antibody, we observed the appearance of high molecular weight Ysh1 species upon addition of recombinant ubiquitin and CPF (Fig. 4A, lane 3) to wild-type extract. These species did not appear when ATP was omitted (Fig. 4A, lane 2) or when methylated ubiquitin (me-ub) was used in the reactions (Fig. 4A, lane 4), or when a reaction was performed without adding Ysh1 (Fig. S1E). ATP is required for the addition of ubiquitin to an active-site cysteine residue on the ubiquitin-activating enzyme [52], and methylation of the ε-amino group of lysines blocks ubiquitin from forming polyubiquitin chains [60]. These results indicate that the larger forms of Ysh1 corresponded to polyubiquitinated Ysh1. When extracts made from *ubc4*$^{\Delta}$ or *mpe1-1* strains were used, the larger species did not form efficiently (Fig. 4B and 4C, lanes 3). However, when recombinant Ubc4 or Mpe1 was added to the reactions, the larger Ysh1 species accumulated, showing that the missing

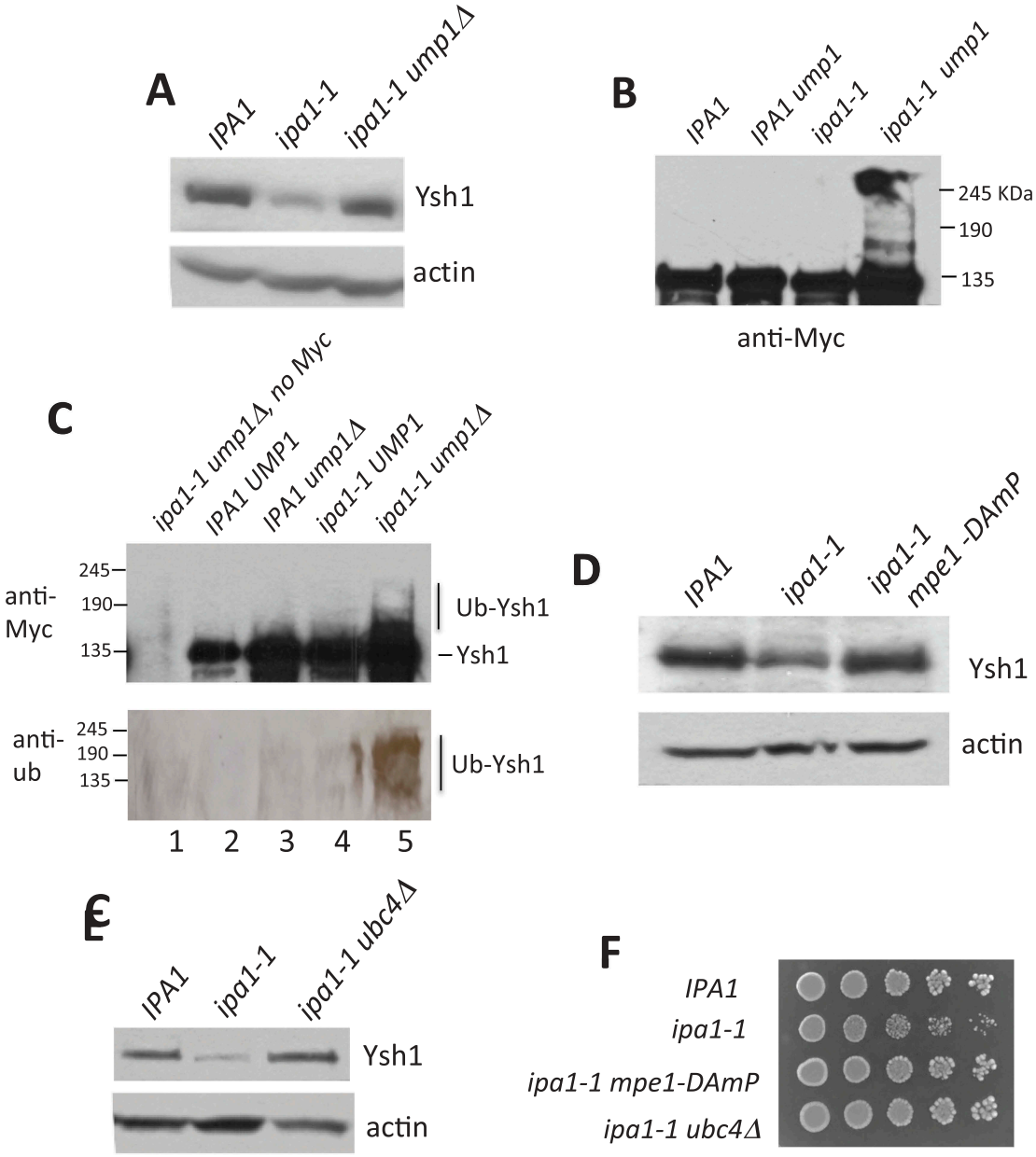

Figure 3. Ysh1 is degraded via the ubiquitin-proteasome system in *ipa1-1*.

(A) *In vivo* expression of Ysh1 in *ipa1-1* and *ipa1-1 ump1*$^{\Delta}$. Cells were grown at 30°C and then shifted to 37°C for 1 hr. Extracts from these cells were analysed by Western blotting using an antibody against Ysh1 or actin. **(B)** Cell lysate prepared from the *ipa1-1 ump1*$^{\Delta}$ cells under denaturing conditions shows higher molecular weight Ysh1 species. Immunoblots were probed with antibody against a Myc tag on Ysh1. **(C)** Ysh1 is ubiquitinated *in vivo* in *ipa1-1*. Ysh1 was immunoprecipitated from the indicated cell extracts. The immunoprecipitate in lane 1 was obtained from *ipa1-1 ump1*$^{\Delta}$ cells with untagged Ysh1. The immunoprecipitates were analysed by Western blotting using antibody against Myc to detect Ysh1 or against ubiquitin. To concentrate the Western signal, a high-percentage acrylamide gel was used for immunoblotting with anti-ubiquitin. **(D, E)** Expression of Ysh1 in the *ipa1-1* mutant or the *ipa1-1* mutant which also contained either a deletion of the *UBC4* gene (*ubc4*$^{\Delta}$) or a mutation of the *MPE1* gene (*mpe1-DAmP*) [39], in which the *MPE1* 3′ UTR is disrupted by insertion of the ampicillin gene, which destabilizes the mRNA, leading to reduced protein expression. Experiments were performed as described in (A). **(F)** Growth of *ipa1-1* relative to *ipa1-1* paired with mutation of *MPE1* or *UBC4*. Cells were grown on YPD plates at 30°C.

factor needed for Ysh1 polyubiquitination in the *ubc4*$^{\Delta}$ or *mpe1-1* extracts was Ubc4 or Mpe1, respectively (Fig. 4B and 4C, lanes 4). Polyubiquitination of Ysh1 was abrogated when me-ub was used instead of ubiquitin (Fig. 4B and 4C, lanes 5).

A purified in vitro system ubiquitinates Ysh1

The data presented above confirm a requirement of Ubc4 and Mpe1 for Ysh1 ubiquitination. We next tested whether Ubc4 and Mpe1 were sufficient to direct Ysh1 ubiquitination by establishing an in vitro ubiquitination assay with purified proteins. His_6-tagged Ubc4 and Mpe1 were expressed in *E. coli* and purified by Ni-chelating affinity chromatography. CPF containing Ysh1-HA_3 was purified from yeast as described above, and recombinant Uba1 (the E1 ubiquitin-activating enzyme) was obtained commercially. When a mixture of Ysh1, Ubc4, Mpe1, Uba1 and ubiquitin was incubated with ATP, Ysh1 was ubiquitinated as shown by the appearance of high molecular

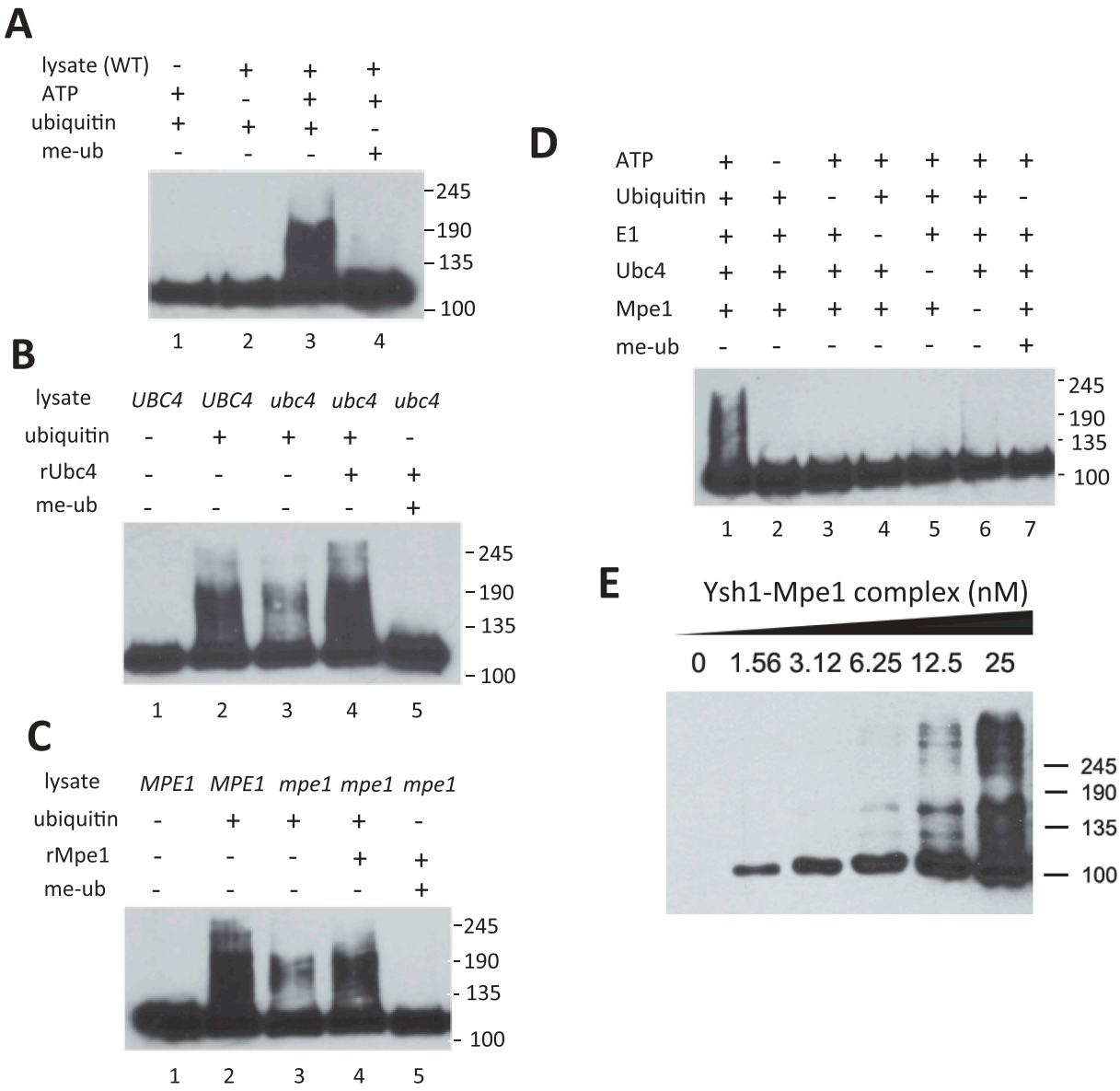

Figure 4. Ubc4 and Mpe1 are required for *in vitro* ubiquitination of Ysh1.

(A) *In vitro* ubiquitination of Ysh1 in cell extract. Extract from wild-type cells was incubated with ubiquitin and CPF purified from yeast expressing 3xHA-TAP-tagged *YSH1*. Components of the in vitro reaction were omitted as indicated, and methylated ubiquitin (me-ub) replaced ubiquitin in lane 4. Ysh1 was detected with HA antibody. **(B)** Lysate prepared from *ubc4Δ* cells does not efficiently ubiquitinate Ysh1 unless recombinant Ubc4 is added. Reactions in lanes 1 and 2 use wild-type extract (*UBC4*). Reactions were performed as described in Panel A, and Ysh1 was detected with HA antibody. **(C)** Lysate prepared from *mpe1-1* cells does not efficiently ubiquitinate Ysh1 unless recombinant Mpe1 is added. Reactions were performed as described in Panel A, and Ysh1 was detected with HA antibody. **(D)** *In vitro* ubiquitination assay with purified proteins. The reaction in lane 1 contains E1 (Uba1), Ubc4, Mpe1, ATP, ubiquitin, and CPF containing Ysh1-HA_3. For lanes 2–7, each component is omitted as indicated, or ubiquitin is replaced with methylated ubiquitin (me-ub). Ysh1 was detected with HA antibody. **(E)** A Ysh1-Mpe1 heterodimer is ubiquitinated in the reconstituted assay. Increasing amounts of the dimer were added as indicated and reactions performed as described in Panel D. In all of the experiments in this figure, marker positions are shown on the right of each panel.

weight species (Fig. 4D, lane 1). When any component was omitted, or when ubiquitin was substituted with me-ubiquitin, these species disappeared, indicating that they correspond to polyubiquitinated Ysh1 (Fig. 4D and Fig. S1F). These data indicate that Ubc4 as a ubiquitin conjugase and Mpe1 as a ubiquitin ligase, along with Uba1 and ubiquitin, are sufficient to mediate Ysh1 ubiquitination.

We also tested whether a Ysh1–Mpe1 complex expressed and purified from insect cells (Fig. S1C) was a substrate for ubiquitination in the reconstituted assay. Ysh1 was readily ubiquitinated when provided in complex with Mpe1, with the ubiquitinated species reaching a larger size than in the previous assay (Fig. 4E), indicating that Ysh1 that is only in complex with Mpe1 is also substrate for ubiquitination.

Our data showing that the Ysh1 level decreased when Ipa1 was depleted (Fig. 1A) suggested that Ipa1 might somehow block Ysh1 ubiquitination and degradation. However, addition of recombinant Ipa1 to the in vitro ubiquitination reaction using cell extract showed no inhibition of ubiquitination in comparison to bovine serum albumin (BSA) added in the same

amounts (Fig. S1G). This finding suggests that Ipa1 is not acting directly to prevent Ubc4 and Mpe1 from modifying Ysh1.

Discussion

Regulating mRNA polyadenylation can help a cell achieve optimal protein production for a given condition or cell state. Because of this potential, a greater knowledge of the fundamental regulatory strategies governing polyadenylation can contribute to understanding of normal cell physiology and dysregulation in the disease state [1]. One mechanism to regulate mRNA polyadenylation is to limit the amount of the core processing machinery, which can contribute to a general decrease in mRNA synthesis when less synthetic capacity is needed. This mechanism can also force favouring of poly(A) sites with better matches to conserved sequence elements on the precursor mRNA, leading to mRNA isoforms with different properties. In this study, we show that the budding yeast protein Ipa1 controls the level of Ysh1, the essential endonuclease that cuts mRNA precursor at the poly-(A) site in preparation for polyadenylation and mRNA nuclear export. Loss of Ipa1 leads to depletion of the Ysh1 protein without affecting *YSH1* mRNA level. Other subunits of the C/P complex are not depleted, indicating selective targeting of Ysh1. We discuss below possible mechanisms by which Ipa1 could act to regulate Ysh1 levels.

Our findings show that increasing the copy number of the *YSH1* gene suppressed the temperature-sensitive growth and the in vivo processing defect of *ipa1-1*, indicating that these defects are largely due to loss of Ysh1. The Ysh1 depletion in *ipa1-1* cells is a consequence of ubiquitin-mediated proteasomal degradation that is facilitated by Mpe1, which, like Ysh1, is an integral subunit of the nuclease module of CPF [40]. Mpe1 possesses a ubiquitin-like domain, a zinc knuckle, and a RING finger domain [34]. Thus, by sequence, Mpe1 is also a member of the RING family of ubiquitin ligases [61], and our results confirm this predicted activity. We have also identified Ubc4 as a ubiquitin conjugase that participates in Ysh1 modification. The sequence of Ipa1 indicates that like Mpe1, it is a ubiquitin ligase, but of the HECT family [41,59]. While Ipa1 possesses homology to the E2 interaction domain of this group of proteins, it does not have an active site cysteine [59], suggesting it does not function like a conventional HECT-type E3, which covalently receives ubiquitin from a partner E2 and transfers it to the target protein.

The molecular mechanism by which Ipa1 prevents Ysh1 degradation is not clear. Biochemical fractionation indicates that while Ipa1 exists in a complex with only the Ysh1 and Mpe1 subunits of CPF, it is not a component of CPF itself [39,40,42]. The direct interaction of Ipa1 with Ysh1 [40] and intracellular presence of the Ipa1/Ysh1/Mpe1 trimer support a role involving physical contact between the two proteins. It is possible that Ipa1, through its interaction with the intrinsically disordered C-terminal domain of Ysh1 [40], protects Ysh1 from degradation until it is incorporated into CPF. However, addition of Ipa1 to an in vitro assay did not block Ysh1 ubiquitination, suggesting Ipa1 is not preventing productive interaction of a ubiquitin conjugase like Ubc4 with the Mpe1/Ysh1 dimer.

Since Ipa1 is found in both nucleus and cytoplasm [59], another role for Ipa1 could be as a co-chaperone to help Ysh1 fold correctly during or after translation (Fig. 5). The Hsp70 and Hsp90 chaperones fold substrate proteins, and accessory proteins called co-chaperones modulate chaperone activity and deliver client proteins [62,63,64]. Ysh1 physically interacts with Hsp82 [65], a member of the Hsp90 family, and several other proteins which assist in protein folding were associated with Ipa1, including Cpr6 and Aha1 (two co-chaperones of Hsp82), the Cct4, Cct6, and Cct8 subunits of the cytosolic Chaperonin Containing TCP1 complex, Hsp42 (a member of the small heat shock chaperone family), Ssa3 (one of the yeast HSP70 ATPases), and Ydj1 (an Ssa3 co-chaperone and Hsp40 family member) [39]. Cells mutated in both *IPA1* and *HSC82*, encoding a paralog of Hsp82, grow more poorly than cells defective for only *IPA1* or *HSC82* [39], suggesting that the two genes lie in compensatory pathways.

Some co-chaperones direct Hsp70/Hsp90 chaperones to participate in either protein degradation or folding [62,63]. Co-chaperones with this activity can be RING-type ubiquitin ligases such as CHIP, and this function has been proposed for the Mpe1 human homolog RBBP6 [66]. Thus, it is

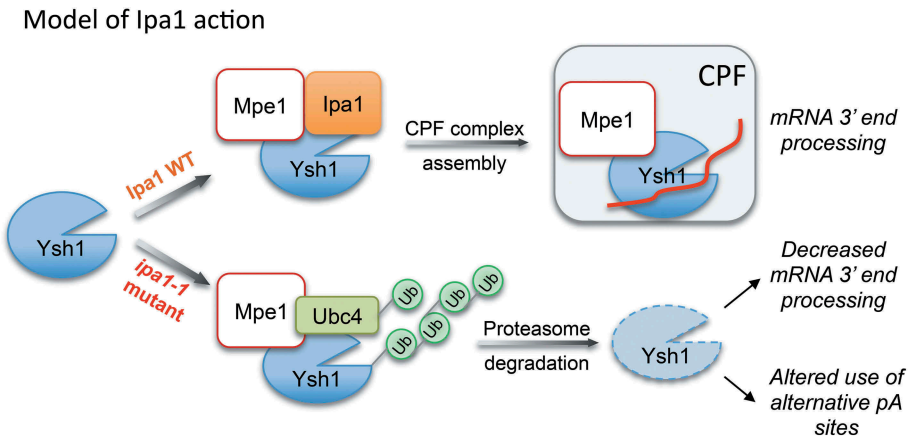

Figure 5. Model for the action of Ipa1 in maintaining the level of Ysh1. In the presence of Ipa1, Ysh1 is correctly folded, and the Ysh1/Mpe1 complex can be incorporated into CPF, leading to efficient mRNA 3′ end processing. In the absence of Ipa1, Ysh1 would not fold properly, leading to ubiquitination and destruction of Ysh1, inefficient mRNA 3′ end processing, and alterations in the choice of the cleavage site.

possible that Ipa1 acts by recruiting a chaperone complex to Ysh1 or otherwise promoting the folding activity of the chaperones. Once folded, the Ysh1/Mpe1 complex could be incorporated into CPF (Fig. 5), through a switch in which Ipa1 interacting at the Ysh1 C-terminal domain is replaced with the CPF Cft2 subunit [40]. In the absence of Ipa1, Ysh1 would not fold properly, leading to ubiquitination and destruction of Ysh1, inefficient mRNA 3′ end processing, and as we described previously, alterations in the choice of poly(A) site position [41]. Our model for Ipa1 action predicts that the Ipa1/Ysh1/Mpe1 complex might be exquisitely tuned for folding or instead, rapid degradation of Ysh1, depending on the needs of the cell. However, we cannot exclude other possible models. For example, Ipa1 could recruit or regulate the abundance of a deubiquitinase that counteracts the activity of Ubc4 and Mpe1 on Ysh1, although there is no evidence for this from reported physical interactions. Ubiquitination does not necessarily lead to degradation [67], and Ipa1 could promote ubiquitination of a factor in a way that regulates its activity towards Ysh1.

Our study suggests that yeast has evolved an easily tunable mechanism that ensures the correct amount of Ysh1 when cells are growing in optimal conditions. It is possible that this mechanism could also allow rapid removal of Ysh1 and a general down-regulation of the polyadenylation capacity of the cell in less favourable growth conditions. Having to modulate only one subunit of the C/P complex (i.e. Ysh1) would provide a means to quickly match this aspect of mRNA synthesis to changing growth conditions. Interestingly, the Ipa1 homolog, UBE3D/UBE2CBP, physically interacts in quantitative proteomics screens with CPSF-73 [68,69], the counterpart of Ysh1. While UBE3D has been implicated in cell cycle regulation [70], age-related macular degeneration [71], the inflammatory condition of aggressive juvenile periodontitis [72], and alterations in the fatty acid profile of muscle [73], its functional role in mammalian cells have not been determined. Future experiments may not only elucidate the precise mechanism by which Ipa1 modulates Ysh1 degradation but also explore whether this regulatory relationship is conserved across eukaryotes.

Materials and methods

Yeast strains and plasmids construction

The *S. cerevisiae* strains used in this study are given in Table 1. SDL98, SDL99, SDL107, and SDL116 were constructed by inserting a Myc13 tag at the C terminus of the endogenous *YSH1* gene as described [74].

For Ysh1 purification in yeast, the*YSH1*-3xHA-TAP (SDL184) strain was constructed using *mpe1-1* (W303a; *ade2-1 ura3-1 his3-11,15 trp1-1 leu2-3,112 can1-100 mpe1-1*) [53], as the host (described below). SDL110 (W303a; *ade2-1 ura3-1 his3-11,15 trp1-1 leu2-3,112 can1-100*)

For pRS315-*YSH1*, the *YSH1* is under the control of the *MPE1* promoter and terminator sequences. The coding sequence of *YSH1* was amplified from genomic DNA by PCR using the upstream primer NdeI-BRR5-fwd (5′ -CTCTACATATG GAGCGAACAAATACAACAACATTC-3′) and the downstream primer NotI-BRR5-rev (5′-tacagGCGGCCGCTTAACATAGC GGTGTGACCAAATTACC-3′). The PCR product was digested with NdeI and NotI and was cloned into the pRS315-*MPE1* vector [34], which was digested with the same restriction enzymes.

Table 1. Yeast strains used in this study.

Strain	Genotype
W303a	*ade2-1 ura3-1 his3-11,15 trp1-1 leu2-3,112 can1-100*
BY4741a	*his3Δ1 leu2Δ0 ura3Δ0 met15Δ0*
SDL164	As BY4741a but *ipa1-1::KanR* [39]
SDL101	As BY4741a but *ipa1-1::KanR, ump1Δ::LEU2* (This study)
SDL89	As BY4741a but *ipa1-1::KanR,ubc4Δ::natR* [39]
SDL90	As BY4741a but *ipa1-1::KanR,mpe1-DAmP::natR* [39]
SDL106	As BY4741a but *ipa1-1::KanR,ubc7Δ::LEU2* [39]
SDL98	As BY4741a but *YSH1*-Myc13::*HisMX6* (This study)
SDL99	As BY4741a but *ipa1-1::KanR,YSH1*-Myc13::*HisMX6* (This study)
SDL107	As BY4741a but *ump1Δ::LEU2,YSH1*-Myc13::*HisMX6* (This study)
SDL116	As BY4741a but *ipa1-1::KanR, ump1Δ::LEU2, YSH1*-Myc13::*HisMX6* (This study)
SDL57	BY4742a; *his3Δ1 leu2Δ0 lys2Δ0 ura3Δ0 ubc4Δ::LEU2*(This study)
SDL110	As W303a but *IPA1*-Myc13::*HisMX6* (This study)
SDL103	As BY4741a but *IPA1*-Myc13::*HisMX6* (This study)
SDL104	As BY4741a but *ipa1-1*-Myc13::*HisMX6* (This study)
mpe1-1	W303a; *ade2-1 ura3-1 his3-11,15 trp1-1 leu2-3,112 can1-100 mpe1-1* [53]

pET21b-MPE1 construction was described in Lee and Moore [34]. For pTD68-Flag-UBC4 construction, DNA sequence containing BamHI-Flag-UBC4-XhoI was ordered as gBlocks from IDT (sequence shown below), digested with BamHI and XhoI, and cloned into pTD68 digested with the same restriction enzymes. The construction of pTD68 was described in Uehara et al. [75]. The *UBC4* sequence (underlined below) was *E.coli* codon optimized.

5′ACTCATGGATCCGACTATAAAGATGACGACGAC-
AAGGGTGGATCGGGCTCGTCTTCTAAGCGCATTGCA-
AAAGAACTGTCTGATCTTGAGCGTGATCCGCCAACG-
TCGTGCTCTGCTGGGCCTGTAGGGGATGATTTGTACC-
ATTGGCAAGCGTCCATCATGGGACCTGCTGACAGTC-
CGTATGCTGGGGGCGTATTTTTTCTTTCCATCCATTT-
TCCGACAGATTACCCTTTTAAGCCCCCTAAGATCTCC-
TTCACCACGAAAATTTACCATCCTAACATCAACGCAA-
ATGGAAACATTTGCCTTGATATCTTAAAGGACCAGTG-
GAGCCCGGCACTTACACTTAGTAAAGTATTGCTTTCT-
ATTTGTTCGTTGCTGACGGACGCCAATCCAGACGATC-
CATTGGTCCCAGAGATCGCTCATATTTACAAGACTGA-
CCGCCCTAAGTACGAAGCGACCGCACGCGAATGGAC-
AAAAAAATATGCCGTCTAACTCGAGTGTCTG3′

For pTD68-V5-IPA1 construction, the same scheme was used as described for pTD68-Flag-*UBC4*. The DNA sequence containing BamHI-V5-IPA1-XhoI was ordered as gBlocks from IDT (sequence shown below). The *IPA1* sequence (underlined below) was *E.coli* codon optimized.

ACTCATGGATCCGGTAAACCAATCCCAAATCCGTT-
ACTTGGGCTTGATTCTACTGGGATGGTACAATACGTA-
GTGGAATGGTTACCACGCATCCAGAGTATCAGCGTT-
GTAGTAGAGGGGTGGAAGCAGGTGGAAATCAAAAAT-
TTGAAAGACACGCTGATGTCCATCTCTGGTGACGAG-
GAGCAGGTAGAAGACATCCTTTTACCCGTTGAAGTA-
GAGGAAAAAGTAGATGCTTCCTATAAATTCAAGAAC-
CGCGGTAAAGACTTGGAGTGGATGACCAAGCTGCGT-

TCCAAAAGCTCGAAGATCTATGATAGCTCGATCATGT-
CACTGCCGGACGGTCGTTGGACAAAGGAGGAGTTGC-
GCTCCGACTCGGACTTCTCTATCGAATGCCTTAATTG-
TAAGCAGAAGATCATTAGCAAAGACAACTGTCAAGT-
TTTGAACGATATGCCGAGCGAATTCTGGTTCGAACTT-
ATGGATTATTGGCACTGCCACAAACCGGATGTAAAA-
GAGGATAAATCTTCATACACGCGCTTTGAGACCCTTA-
AACCGTCCAAAAATGAAATTCTTATTGGGTCTTCCTA-
TTTCCAAGGCACTCCTGCGACGTTTGAAAACGTAGCA-
ACGACGAAAGAAAATGACAATGTTCTGTGCATCAAA-
TGTTCAGCTGTGCTTGGACAAGTTACTGCAGGTAGCT-
TATACAAGCTTCACAAGTGGAAACTGCAATTAATCCG-
TTCAGGAAACACATACAAGTTCCCTCCCGAATGTGAT-
ATTACCATCTCATTAATTAATGTAGTTAAAGCGAATT-
CCTGCCGCTATGTTCTGGTGAAATGCAAAACTGAAA-
GTTTACTGGTCTGGATCTTTAGTGTGGACATCGGAGT-
TACTTTGACGGGAAACAAATCGTTCAAACGTGCGAT-
GAAGCTGCTTTACACTAATTCTGTCACTACAATCAAC-
CGCTGCCTTAATCGCCAAGTGGTAGAGGAGTTGGAC-
TTCCAGGAAACCTCGTTTAACGCATTCTATTCCGCCT-
TGCAACATACAAATGCTTTGCTTCCATCGAGTATGAA-
AAAAATTGGGGAGTGGACAATTTCATATACCTCGCTT-
ATCTAACTCGAGTGTCTG

The *YSH1*-3xHA-TAP in *mpe1-1* background was generated by inserting the 3xHA-TAP sequence immediately upstream of the stop codon of *YSH1* as previously described with some modifications [76]. In brief, 3xHA-TAP-*TRP1* bracketed by sequences flanking the *YSH1* stop codon was amplified by PCR with pBS1479 as a template by using Q5 High-Fidelity DNA polymerase (NEB) and primers BRR5-3HA-TAP-fwd (5′-AGGGTGGAAAGCCTCTTAAATATTG GTGGTAATTTGGTCACACCGCTATGTGGATCCGGTTC-TTTAATTAACATCTTTTACCCATACGATGTTCCTGAC-TATGCGGGCTATCCGTATGACGTCCCGGACTATGCA-GGATCCTATCCATATGACGTTCCAGATTACGCTGCTC-AGTGCGGAGGATCCATGGAAAAGAGAAG-3′) and BR R5-3HA-TAP-rev (5′-CGTAAAGAGTGATTAAGGTAAAC AATAAAAGGCAGTTCTAACCAGATTTTGGTTTGGTAT-TACTTCTATAAAGTAGTCTACTTAGTATGCGTAACTG-TTTtacgactcactataggg-3′). Each primer has a pBS1479 specific sequence (underlined) and a 50-base (fwd primer) and 100-base (reverse primer) *YSH1*-specific sequence. *mpe1-1* cells were transformed with the *YSH1*-3xHA-TAP-*TRP1* PCR product, followed by selection for the *TRP1* marker. Transformants harbouring *YSH1*-3xHA-TAP-*TRP1* were verified by PCR and the expression of *YSH1*-3xHA-TAP was confirmed by Western blot.

Yeast spot assay and cultures

Growth properties were analysed by growing strains in liquid yeast extract-peptone-dextrose (YPD) at room temperature to an optical density at 600 nm (OD_{600}) of 1.0, spotting 5 of 10-fold serial dilutions onto YPD plates, and incubating the plates for 3 days at 30°C or 37°C.

Affinity purification of Ysh1-3HA-TAP and PTA1-TAP

Yeast expressing 3xHA-TAP-tagged *YSH1* in the *mpe1-1* background [53] were grown in 8 L of YPD at 25°C to an OD_{600} = 0.7 and shifted to 37°C for 1.5 h. For purification of CPF, FY23 cells carrying *PTA1*-TAP [22] were grown in 8 L of YPD at 30°C to an OD_{600} = 1.0. Extracts were prepared as described previously [77] except omitting the ammonium sulphate precipitation step. CPF was purified according to the standard TAP procedure [76] except that the IgG beads were washed with high salt buffer (1.5 M NaCl) for CPF used in the in vitro ubiquitination assays. The eluates were separated on an SDS-8% polyacrylamide gel and detected by silver staining (Fig. S1B). Ysh1 was confirmed by Western blot analysis using anti-HA antibody.

Preparation of extracts and in vitro mRNA 3′ end processing assays

Preparation of yeast processing extracts and processing assays were done as described previously [77]. For the rescue experiment with TAP-purified CPF, 10–30 ng of CPF was mixed with yeast extracts and incubated for 5 min at 25°C before RNA substrate was added. Western blotting to determine levels of proteins in the processing extracts was performed according to standard procedures. The monoclonal antibodies against Pta1 and Pap1 have been described previously [77]. Polyclonal antibodies against Rna14 and Rna15, and Ysh1 were a gift from H. Domdey. Polyclonal antibody against Mpe1 was a gift from F. Wyers. The antibodies against Ssu72, Pfs2, Fip1, and Yth1 have been described previously [5].

Co-immunoprecipitation assays

Yeast processing extracts (1 mg) prepared as described previously [77] were incubated with anti-Pap1 antibody overnight at 4°C in 500 µl of buffer IP-150 (10 mM Tris-HCl at pH 7.9, 150 mM NaCl, 1 mM EDTA, 10% glycerol, 1 mM dithiothreitol [DTT], 1 mM phenylmethylsulfonyl fluoride [PMSF], 2 µM pepstatin A, 0.6 µM leupeptin, 0.05% NP-40). IP samples were then incubated with protein G beads for 1 hr at 4°C, washed 5X with 1 ml of buffer IP-150, and eluted with 70 µl of SDS sample buffer (without reducing reagent) for 15 min at 25°C. The eluates were resuspended with SDS sample buffer, boiled for 3 min, and analysed in an SDS-10% polyacrylamide gel.

In vivo detection of Ysh1 ubiquitination

The method for purifying ubiquitinated proteins under denaturing conditions was described previously by Laney and Hochstrasser [78]. For our experiments, cells were grown in 20 ml of minimal medium at 30°C to an OD_{600} = 0.5 and shifted to 37°C for 1 hour. Cells were resuspended in 200 µl SDS buffer (2% SDS and 45 mM HEPES, pH 7.5), boiled for

15 min, and centrifuged at 14,000 x g for 5 min. The supernatant was diluted with 4 ml ice-cold Triton lysis buffer (1% Triton X-100, 150 mM NaCl, 50 mM HEPES, pH 7.5, 5 mM EDTA, 20 mM NEM, 1 mM 1,10-phenanthroline monohydrate, 1 mM PMSF, 2 μM pepstatin A, and 0.6 μM leupeptin) and incubated with anti-Myc antibody for 30 min at 4° C. Protein G beads (Santa Cruz) were then added and rotated for another 30 min. Beads were washed three times with 1 ml Triton lysis buffer containing 0.05% SDS, resuspended in SDS sample buffer, boiled for 5 min, and analysed in an SDS-PAGE. Western blotting was performed according to standard procedures except that after transfer, the nitrocellulose membrane was submerged in water and autoclaved for 40 min to improve immuno-detection of ubiquitin, blocked with 5% bovine serum albumin, and then probed with anti-ubiquitin from Santa Cruz (sc-8017). For detection of Ysh1, anti-Myc antibody (9E10) was used.

Recombinant protein expression and purification

Mpe1 was expressed and purified from *E. coli* Rosetta (DE3) cells according to Lee and Moore [34]. Recombinant Ubc4 and Ipa1 were expressed and purified from *E. coli* Rosetta cells as in Cho et al. [79] with the following exceptions. Buffer A was composed of 50 mM sodium phosphate buffer, pH 8.0, 300 mM NaCl, 10 mM Imidazole, 5% glycerol, 5 mM β-mercaptoethanol, 1 mM phenylmethylsulfonyl fluoride [PMSF], 2 μM pepstatin A, and 0.6 μM leupeptin. Buffer B was composed of 50 mM sodium phosphate buffer, pH 8.0, 150 mM NaCl, 1 mM phenylmethylsulfonyl fluoride (PMSF), 2 μM pepstatin A, and 0.6 μM leupeptin. Ipa1-His_6 was expressed from a pET21a plasmid, and protein purified by nickel affinity chromatography. Ubc4 was expressed from the pTD68 plasmid [75], which adds a His_6-SUMO-FLAG tag to the N-terminus of Ubc4, and purified as described in Uehara, et al. [75]. After purification of the Ubc4 fusion protein by nickel-affinity chromatography, the His_6-SUMO tag was released using His_6-tagged SUMO protease. Cleavage reactions were passed through Ni-NTA resin to remove free H-SUMO and the protease. The purified proteins (Fig. S1D) were dialysed against buffer D (50 mM Tris, pH 7.9, 150 mM NaCl, 0.5 mM DTT, 20% glycerol, 1 mM phenylmethylsulfonyl fluoride (PMSF), 2 μM pepstatin A, and 0.6 μM leupeptin).

For expression of the Ysh1–Mpe1 complex in Sf9 insect cells, we used Bac-to-Bac technology (Thermo Fisher) as described by Cooper et al. [80]. The Mpe1 ORF tagged with Myc (5′) and His6 (3′) was inserted into pFastBac-Dual after the pPolh promoter using the SacI and NotI sites, and the Ysh1 ORF tagged with His6 (5′) and 3HA (3′) was inserted into pFastBac-Dual after the p10 promoter using the XhoI and NheI sites. The pFASTbac-Dual-Ysh1-Mpe1 recombinant plasmid was validated by Sanger sequencing. The construct was transformed into DH10Bac cells and positive colonies were selected by Bluo-Gal. Bacmid DNA was prepared by using the P1, P2 and N3 buffer from Qiagen miniprep kit (Cat. No. 27106) followed by isopropanol precipitation. The purified bacmid DNA was used for transfection in Sf9 insect cell to make baculovirus.

For expression and purification of the Ysh1–Mpe1 complex, Sf9 cells were grown in Sf900-SFM medium (Thermo Fisher) to a density of 2×10^6 cells/ml and infected with recombinant baculovirus by adding 7.5 ml of the viral stock from the third passage (P3) to 1.5 litres of cells in a 5-litre incubation bottle. Seventy-two hours after infection, cells were harvested and resuspended in solubilization buffer (50 mM Tris-HCl, pH 8.0, 150 mM NaCl, 10 mM imidazole, 10% glycerol, 10 uM pepstatin A, 100 uM leupeptin and 1 mM PMSF). The suspension was lysed by passing it three times through an M-110S microfluidizer according to the manufacturer's instructions. Supernatant was collected from lysate by centrifugation at 4,000 g for 25 min. Ysh1 and Mpe1 in 45 mL of supernatant were isolated by adding 1 mL Ni Superflow resin (GE Healthcare). After incubation for 1 h, the resin was washed three times with 15 column volumes of 50 mM Tris pH 8.0, 150 mM NaCl and 10 mM imidazole. Ysh1 and Mpe1 were eluted with 50 mM Tris pH 8.0, 150 mM NaCl, and 300 mM imidazole and concentrated in a centrifuge filter (molecular weight cut-off of 30 kDa, Millipore EMD). Ysh1–Mpe1 complex was further purified by anti-HA beads (Thermo Fisher, #26181) according to the manufacture instructions and analysed by coomassie blue staining and Western Blot using anti-HA antibody (sc-7392) and Anti-MYC antibody (sc-40) from Santa Cruz (Fig. S1C). The concentrations of purified proteins were determined by BCA protein assay (Thermo Fisher).

In vitro ubiquitination assays

Yeast crude extracts were prepared as described in Zhao et al. [77]. The extracts are diluted to 1 μg/μl in buffer D (50 mM Tris, pH 7.9, 150 mM NaCl, 0.5 mM DTT, 20% glycerol, 1 mM phenylmethylsulfonyl fluoride [PMSF], 2 μM pepstatin A, and 0.6 μM leupeptin). The reaction includes 2 μg of extract, 2 μl of 5X reaction buffer (100 mM Tris pH 7.5, 100 mM $MgCl_2$, 10 mM ATP, and 5 mM DTT), 15 μM ubiquitin aldehyde (Boston Biochem U-201), 0.2 mM ubiquitin (Boston Biochem U-100sc) or 0.2 mM me-ubiquitin (Boston Biochem U-501), and the CPF-high-salt fraction in a final volume of 10 μl. For recombinant Ubc4 and Mpe1 add-back experiments, protein was added to 1.5 μM in a final volume of 10 μl. These reactions were carried out at 37°C for 10 min. The reactions with purified components shown in Fig. 3D include 10 nM Uba1 (Boston Biochem E-300), 200 nM Ubc4, 200 nM Mpe1, 0.2 mM ubiquitin or 0.2 mM me-ubiquitin and ~200 nM Ysh1-high-salt fraction and 2 μl of 5X reaction buffer (same as above) in a final volume of 10 μl. These reactions were carried out at 30°C for 20 min. The in vitro ubiquitination assays (total reaction volume of 20 μL) shown in Fig. 3E were performed using Uba1 (125 nM), Ubc4 (500 nM), 1 μg/μL ubiquitin, the Ysh1–Mpe1 complex expressed in insect cells at the indicated concentrations in 100 mM Tris, pH 7.5, 100 mM $MgCl_2$, 10 mM ATP, 4 mM MgCl2, and 5 mM DTT for 30 min at 30°C. Reactions were stopped by addition of SDS sample buffer containing 4% β-mercaptoethanol, heated at 95°C for 5 min, and resolved on 10% Bis-Tris gels or by SDS-PAGE followed by immunoblotting with the indicated antibodies.

Table 2. Primers used for RT-qPCR.

Primer Name	Primer Sequence 5′-3′
PDC1 Forward	GCCAGTCTTCGATGCTCCAC
PDC1 Total Reverse	ATCGCTTATTGCTTAGCGTTGG
PDC1 pA Span Reverse	ACTGTCGGCAACTTCTTGTCTGG
RPP1B Total Forward	ACGCTAAGGCTTTGGAAGGTAAGGA
RPP1B Total Reverse	AACCGAAACCCATGTCGTCGTCAGA
RPP1B pA Span Forward	GACGACGACATGGGTTTCGGT
RPP1B pA Span Reverse	TCGTAGCCCTTTCGTATGGACA

qRT-PCR analysis

Total RNA from wild-type or mutant cells was isolated using the Hot Phenol Method [81] and Heavy Phase Lock Gel tubes (Quantabio), and treated with RQ1 DNase (Promega). DNA-free RNA was subjected to reverse transcription using random hexamers. The resulting cDNA samples were analysed using real-time PCR analysis performed in a 12 µl reaction with 0.5 µl of 10 µM forward and reverse primers, 5 µl of SYBR Green Supermix (BIO-RAD), 1 µl cDNA, and 5 µl of distilled water. The primer sequences are listed in Table 2. The expression of the unprocessed transcript of a given gene was normalized to the expression of total mRNA of that gene.

Global gene expression analysis

RNA sequencing data sets for the *ipa1-1, pcf11-2* and *cft2-1* were obtained from Costanzo et al. [39] and processed and analysed as described previously for the *ipa1-1* data set [41]. Differential expression assessment was made with DESeq2 [80], using a threshold of $\log_2$ fold-change > 0.5, p-value < 0.2 for increased genes, or $\log_2$ fold-change < 0.5, p-value < 0.2 for decreased genes, and based only upon poly(A) site tags that supported a full-length mRNA transcript. Venn diagrams were generated with eulerr [50]. Cumulative polyadenylation distribution (CPD) plots were determined as described in Graber et al. [5].

Acknowledgments

We thank members of the laboratories of C. Moore and A. Bohm for critical input regarding our experiments and manuscript and to Ellen White and Katya Heldwein for help with protein expression in insect cells. We are grateful to A. Greenleaf, D. Bentley, H. Domdey, M. Hampsey, M. Henry, and F. Lacroute for the generous gifts of antibodies used in this study. This work was supported by NSF grant MCB-1244043 to C. Moore. J. Graber was partially supported by an Institutional Development Award (IDeA) from the National Institute of General Medical Sciences of the National Institutes of Health under grant numbers P20GM103423 and P20GM104318.

Disclosure statement

No potential conflict of interest was reported by the authors.

Funding

This work was supported by the National Institutes of Health [P20GM103423 and P20GM104318];National Science Foundation [MCB-1244043];

ORCID

Joel H. Graber http://orcid.org/0000-0001-5137-4553
Daniel Heller-Trulli http://orcid.org/0000-0003-0549-0646
Katarzyna Kaczmarek Michaels http://orcid.org/0000-0002-2525-5830
Claire L. Moore http://orcid.org/0000-0002-1883-9459

References

[1] Gruber AJ, Zavolan M. Alternative cleavage and polyadenylation in health and disease. Nat Rev Genet. 2019;20:599–614.
[2] Mayr C. Regulation by 3′-Untranslated Regions. Annu Rev Genet. 2017;51:171–194.
[3] Chen M, Lyu G, Han M, et al. 3′ UTR lengthening as a novel mechanism in regulating cellular senescence. Genome Res. 2018;28:285–294.
[4] de Lorenzo L, Sorenson R, Bailey-Serres J, et al. Noncanonical alternative polyadenylation contributes to gene regulation in response to hypoxia. Plant Cell. 2017;29:1262–1277.
[5] Graber JH, Nazeer FI, Yeh PC, et al. DNA damage induces targeted, genome-wide variation of poly(A) sites in budding yeast. Genome Res. 2013;23:1690–1703.
[6] Jia X, Yuan S, Wang Y, et al. The role of alternative polyadenylation in the antiviral innate immune response. Nat Commun. 2017;8:14605.
[7] MacDonald CC. Tissue-specific mechanisms of alternative polyadenylation: testis, brain, and beyond (2018 update). Wiley Interdiscip Rev RNA. 2019;10:e1526.
[8] Neve J, Patel R, Wang Z, et al. Cleavage and polyadenylation: ending the message expands gene regulation.s. RNA Biology. 2017;14:865–890.
[9] Pai AA, Baharian G, Page Sabourin A, et al. Widespread shortening of 3′ untranslated regions and increased exon inclusion are evolutionarily conserved features of innate immune responses to infection. PLoS Genet. 2016;12:e1006338.
[10] Shi Y, Manley JL. The end of the message: multiple protein-RNA interactions define the mRNA polyadenylation site. Genes Dev. 2015;29:889–897.
[11] Tang S, Patel A, Krause PR. Herpes simplex virus ICP27 regulates alternative pre-mRNA polyadenylation and splicing in a sequence-dependent manner. Proc Natl Acad Sci U S A. 2016;113:12256–12261.
[12] Tian B, Manley JL. Alternative polyadenylation of mRNA precursors. Nat Rev Mol Cell Biol. 2017;18:18–30.
[13] Yoon OK, Brem RB. Noncanonical transcript forms in yeast and their regulation during environmental stress. RNA. 2010;16:1256–1267.
[14] Zheng D, Wang R, Ding Q, et al. Cellular stress alters 3′UTR landscape through alternative polyadenylation and isoform-specific degradation. Nat Commun. 2018;9:2268.
[15] Masamha CP, Wagner EJ. The contribution of alternative polyadenylation to the cancer phenotype. Carcinogenesis. 2018;39:2–10.
[16] Park HJ, Ji P, Kim S, et al. 3′ UTR shortening represses tumor-suppressor genes in trans by disrupting ceRNA crosstalk. Nat Genet. 2018;50:783–789.
[17] Sadek J, Omer A, Hall D, et al. Alternative polyadenylation and the stress response. Wiley Interdiscip Rev RNA. 2019;10:e1540.
[18] Elkon R, Ugalde AP, Agami R. Alternative cleavage and polyadenylation: extent, regulation and function. Nat Rev Genet. 2013;14:496–506.
[19] Mizrahi N, Moore C. Posttranslational phosphorylation and ubiquitination of the *Saccharomyces cerevisiae* Poly(A) polymerase at the S/G(2) stage of the cell cycle. Mol Cell Biol. 2000;20:2794–2802.
[20] Colgan DF, Murthy KG, Zhao W, et al. Inhibition of poly(A) polymerase requires p34cdc2/cyclin B phosphorylation of multiple consensus and non-consensus sites. Embo J. 1998;17:1053–1062.
[21] Kim H, Lee JH, Lee Y. Regulation of poly(A) polymerase by 14-3-3epsilon. Embo J. 2003;22:5208–5219.

[22] He X, Moore C. Regulation of yeast mRNA 3′ end processing by phosphorylation. Mol Cell. 2005;19:619–629.
[23] Ryan K. Pre-mRNA 3′ cleavage is reversibly inhibited in vitro by cleavage factor dephosphorylation. RNA Biol. 2007;4:26–33.
[24] Tang HW, Hu Y, Chen CL, et al. The TORC1-regulated CPA complex rewires an RNA processing network to drive autophagy and metabolic reprogramming. Cell Metab. 2018;27:1040–54 e8.
[25] Kajitani N, Glahder J, Wu C, et al. hnRNP L controls HPV16 RNA polyadenylation and splicing in an Akt kinase-dependent manner. Nucleic Acids Res. 2017;45:9654–9678.
[26] Dermody JL, Dreyfuss JM, Villen J, et al. Unphosphorylated SR-like protein Npl3 stimulates RNA polymerase II elongation. PloS One. 2008;3:e3273.
[27] Shimazu T, Horinouchi S, Yoshida M. Multiple histone deacetylases and the CREB-binding protein regulate pre-mRNA 3′-end processing. J Biol Chem. 2007;282:4470–4478.
[28] Richard P, Vethantham V, Manley JL. Roles of sumoylation in mRNA processing and metabolism. Adv Exp Med Biol. 2017;963:15–33.
[29] Xiang K, Tong L, Manley JL. Delineating the structural blueprint of the pre-mRNA 3′-end processing machinery. Mol Cell Biol. 2014;34:1894–1910.
[30] Kumar A, Clerici M, Muckenfuss LM, et al. Mechanistic insights into mRNA 3′-end processing. Curr Opin Struct Biol. 2019;59:143–150.
[31] Kamieniarz-Gdula K, Gdula MR, Panser K, et al. Selective roles of vertebrate PCF11 in premature and full-length transcript termination. Mol Cell. 2019;74:158–172.
[32] Rehfeld A, Plass M, Krogh A, et al. Alterations in polyadenylation and its implications for endocrine disease. Front Endocrinol (Lausanne). 2013;4:53.
[33] Shell SA, Hesse C, Morris SM Jr., et al. Elevated levels of the 64-kDa cleavage stimulatory factor (CstF-64) in lipopolysaccharide-stimulated macrophages influence gene expression and induce alternative poly(A) site selection. J Biol Chem. 2005;280:39950–39961.
[34] Lee SD, Moore CL. Efficient mRNA polyadenylation requires a ubiquitin-like domain, a zinc knuckle, and a RING finger domain, all contained in the Mpe1 protein. Mol Cell Biol. 2014;34:3955–3967.
[35] Mandel CR, Kaneko S, Zhang H, et al. Polyadenylation factor CPSF-73 is the pre-mRNA 3′-end-processing endonuclease. Nature. 2006;444:953–956.
[36] Eaton JD, Davidson L, Bauer DLV, et al. Xrn2 accelerates termination by RNA polymerase II, which is underpinned by CPSF73 activity. Genes Dev. 2018;32:127–139.
[37] Baejen C, Andreani J, Torkler P, et al. Genome-wide analysis of RNA Polymerase II termination at protein-coding genes. Mol Cell. 2017;66:38–49.
[38] Schaughency P, Merran J, Corden JL. Genome-wide mapping of yeast RNA polymerase II termination. PLoS Genet. 2014;10:e1004632.
[39] Costanzo M, VanderSluis B, Koch EN, et al. A global genetic interaction network maps a wiring diagram of cellular function. Science. 2016;353(6306).
[40] Hill CH, Boreikaite V, Kumar A, et al. Activation of the endonuclease that defines mRNA 3′ ends requires incorporation into an 8-subunit core cleavage and polyadenylation factor complex. Mol Cell. 2019;73:1217–1231.
[41] Pearson EL, Graber JH, Lee SD, et al. Ipa1 is an RNA polymerase II elongation factor that facilitates termination by maintaining levels of the poly(A) site endonuclease Ysh1. Cell Rep. 2019;26:1919–1933.
[42] Casanal A, Kumar A, Hill CH, et al. Architecture of eukaryotic mRNA 3′-end processing machinery. Science. 2017;358:1056–1059.
[43] Lidschreiber M, Easter AD, Battaglia S, et al. The APT complex is involved in non-coding RNA transcription and is distinct from CPF. Nucleic Acids Res. 2018;46:11528–11538.
[44] He X, Khan AU, Cheng H, et al. Functional interactions between the transcription and mRNA 3′ end processing machineries mediated by Ssu72 and Sub1. Genes Dev. 2003;17:1030–1042.
[45] Ghazy MA, He X, Singh BN, et al. The essential N terminus of the Pta1 scaffold protein is required for snoRNA transcription termination and Ssu72 function but is dispensable for pre-mRNA 3′-end processing. Mol Cell Biol. 2009;29:2296–2307.
[46] Preker PJ, Lingner J, Minvielle-Sebastia L, et al. The FIP1 gene encodes a component of a yeast pre-mRNA polyadenylation factor that directly interacts with poly(A) polymerase. Cell. 1995;81:379–389.
[47] Ohnacker M, Barabino SM, Preker PJ, et al. The WD-repeat protein pfs2p bridges two essential factors within the yeast pre-mRNA 3′-end-processing complex. Embo J. 2000;19:37–47.
[48] Dominski Z, Yang XC, Purdy M, et al. A CPSF-73 homologue is required for cell cycle progression but not cell growth and interacts with a protein having features of CPSF-100. Mol Cell Biol. 2005;25:1489–1500.
[49] Ramos PC, Hockendorff J, Johnson ES, et al. Ump1p is required for proper maturation of the 20S proteasome and becomes its substrate upon completion of the assembly. Cell. 1998;92:489–499.
[50] Oliveros JC An interactive tool for comparing lists with Venn's diagrams. 2007-2015. http://bioinfogp.cnb.csic.es/tools/venny/index.html
[51] Zheng N, Shabek N. Ubiquitin ligases: structure, function, and regulation. Annu Rev Biochem. 2017;86:129–157.
[52] Varshavsky A. The ubiquitin system, an immense realm. Annu Rev Biochem. 2012;81:167–176.
[53] Vo LT, Minet M, Schmitter JM, et al. Mpe1, a zinc knuckle protein, is an essential component of yeast cleavage and polyadenylation factor required for the cleavage and polyadenylation of mRNA. Mol Cell Biol. 2001;21:8346–8356.
[54] Chibi M, Meyer M, Skepu A, et al. RBBP6 interacts with multifunctional protein YB-1 through its RING finger domain, leading to ubiquitination and proteosomal degradation of YB-1. J Mol Biol. 2008;384:908–916.
[55] Di Giammartino DC, Li W, Ogami K, et al. RBBP6 isoforms regulate the human polyadenylation machinery and modulate expression of mRNAs with AU-rich 3′ UTRs. Genes Dev. 2014;28:2248–2260.
[56] Finley D, Ulrich HD, Sommer T, et al. The ubiquitin-proteasome system of *Saccharomyces cerevisiae*. Genetics. 2012;192:319–360.
[57] Matsuo Y, Ikeuchi K, Saeki Y, et al. Ubiquitination of stalled ribosome triggers ribosome-associated quality control. Nat Commun. 2017;8:159.
[58] Singh RK, Gonzalez M, Kabbaj MH, et al. Novel E3 ubiquitin ligases that regulate histone protein levels in the budding yeast *Saccharomyces cerevisiae*. PloS One. 2012;7:e36295.
[59] Lutz AP, Schladebeck S, Renicke C, et al. Proteasome activity is influenced by the HECT_2 protein Ipa1 in budding yeast. Genetics. 2018;209:157–171.
[60] Hershko A, Heller H. Occurrence of a polyubiquitin structure in ubiquitin-protein conjugates. Biochem Biophys Res Commun. 1985;128:1079–1086.
[61] Metzger MB, Pruneda JN, Klevit RE, et al. RING-type E3 ligases: master manipulators of E2 ubiquitin-conjugating enzymes and ubiquitination. Biochim Biophys Acta. 2014;1843:47–60.
[62] Edkins AL. CHIP: a co-chaperone for degradation by the proteasome. Subcell Biochem. 2015;78:219–242.
[63] Rosenzweig R, Nillegoda NB, Mayer MP, et al. The Hsp70 chaperone network. Nat Rev Mol Cell Biol. 2019;20:665–680.
[64] Nathan DF, Vos MH, Lindquist S. In vivo functions of the *Saccharomyces cerevisiae* Hsp90 chaperone. Proc Natl Acad Sci U S A. 1997;94:12949–12956.
[65] Zhao R, Davey M, Hsu YC, et al. Navigating the chaperone network: an integrative map of physical and genetic interactions mediated by the hsp90 chaperone. Cell. 2005;120:715–727.
[66] Kappo MA, Ab E, Hassem F, et al. Solution structure of RING finger-like domain of retinoblastoma-binding protein-6 (RBBP6)

suggests it functions as a U-box. J Biol Chem. 2012;287:7146–7158.
[67] Yau R, Rape M. The increasing complexity of the ubiquitin code. Nat Cell Biol. 2016;18:579–586.
[68] Hein MY, Hubner NC, Poser I, et al. A human interactome in three quantitative dimensions organized by stoichiometries and abundances. Cell. 2015;163:712–723.
[69] Huttlin EL, Bruckner RJ, Paulo JA, et al. Architecture of the human interactome defines protein communities and disease networks. Nature. 2017;545:505–509.
[70] Kobirumaki F, Miyauchi Y, Fukami K, et al. A novel UbcH10-binding protein facilitates the ubiquitinylation of cyclin B in vitro. J Biochem. 2005;137:133–139.
[71] Huang LZ, Li YJ, Xie XF, et al. Whole-exome sequencing implicates UBE3D in age-related macular degeneration in East Asian populations. Nat Commun. 2015;6:6687.
[72] Offenbacher S, Divaris K, Barros SP, et al. Genome-wide association study of biologically informed periodontal complex traits offers novel insights into the genetic basis of periodontal disease. Hum Mol Genet. 2016;25:2113–2129.
[73] Rovadoscki GA, Pertile SFN, Alvarenga AB, et al. Estimates of genomic heritability and genome-wide association study for fatty acids profile in santa ines sheep. BMC Genomics. 2018;19:375.
[74] Longtine MS, McKenzie A 3rd, Demarini DJ, et al. Additional modules for versatile and economical PCR-based gene deletion and modification in saccharomyces cerevisiae. Yeast. 1998;14:953–961.
[75] Uehara T, Parzych KR, Dinh T, et al. Daughter cell separation is controlled by cytokinetic ring-activated cell wall hydrolysis. Embo J. 2010;29:1412–1422.
[76] Puig O, Caspary F, Rigaut G, et al. The tandem affinity purification (TAP) method: a general procedure of protein complex purification. Methods. 2001;24:218–229.
[77] Zhao J, Kessler M, Helmling S, et al. Pta1, a component of yeast CF II, is required for both cleavage and poly(A) addition of mRNA precursor. Mol Cell Biol. 1999;19:7733–7740.
[78] Laney JD, Hochstrasser M. Analysis of protein ubiquitination. Curr Protoc Protein Sci. 2011;66. Chapter 14:Unit145:14.5.1–14.5.13.
[79] Cho H, McManus HR, Dove SL, et al. Nucleoid occlusion factor SlmA is a DNA-activated FtsZ polymerization antagonist. Proc Natl Acad Sci U S A. 2011;108:3773–3778.
[80] Cooper RS, Georgieva ER, Borbat PP, et al. Structural basis for membrane anchoring and fusion regulation of the herpes simplex virus fusogen gB. Nat Struct Mol Biol. 2018;25:416–424.
[81] Ares M. Isolation of total RNA from yeast cell cultures. Cold Spring Harb Protoc. 2012;2012:1082–1086.